Regulation of P-glycoprotein and Breast Cancer Resistance Protein Expression Induced by Focused Ultrasound-Mediated Blood-Brain Barrier Disruption: A Pilot Study

Allegra Conti, Francoise Geffroy, Hermes Kamimura, Anthony Novell, Nicolas Tournier, Sébastien Mériaux, Benoit Larrat

International Journal of *Molecular Sciences*

MDPI

Article

Regulation of P-glycoprotein and breast cancer resistance protein expression induced by focused ultrasound-mediated blood-brain barrier disruption: a pilot study

Allegra Conti [1,2]*, Francoise Geffroy [1], Hermes A. S. Kamimura [1], Anthony Novell [3], Nicolas Tournier [3], Sébastien Mériaux [1] and Benoit Larrat [1]

[1] NeuroSpin/ Institut des sciences de la vie Frédéric Joliot / Direction de la recherche Fondamentale /Commissariat à l'Energie Atomique et aux Energies Alternatives, Université Paris Saclay, Gif-sur-Yvette, France
[2] Department of Biomedicine and Prevention, University of Rome Tor Vergata, Rome, Italy;
[3] Université Paris-Saclay, CEA, CNRS, Inserm, BioMaps, Orsay, France
* Correspondence: allegra.conti@uniroma2.it

Abstract: The blood-brain barrier (BBB) controls brain homeostasis, and it is formed by vascular endothelial cells, physically connected by tight junctions (TJs). The BBB expresses efflux transporters such as the P-glycoprotein (P-gp) and the breast cancer resistance protein (BCRP), which limit the passage of substrate molecules from the circulation to the brain. Focused ultrasound (FUS) with microbubbles can create a local and reversible detachment of TJs. However, very little is known about the effect of FUS on the expression of efflux transporters. We investigated in vivo the effects of moderate acoustic pressures on both P-gp and BCRP expressions up to 2 weeks after sonication. Magnetic resonance-guided FUS was applied in the striatum of 12 rats. P-gp and BCRP expression were determined by immunohistochemistry at 1, 3, 7, and 14 days post-FUS. Our results indicate that FUS-induced BBB opening is capable of i) decreasing P-gp expression up to 3 days after sonication, both in the treated and in the contralateral brain regions, and ii) overexpressing BCRP up to 7 days after FUS in sonicated regions only. Our findings may help improve FUS-aided drug delivery strategies by considering both the mechanical effect on the TJs and the regulation of P-gp and BCRP.

Keywords: Focused ultrasound; BBB-opening; Efflux transporter; MRgFUS; Drug delivery

Citation: Conti, A.; Geffroy, F.; Kamimura, H. A. S.; Novell, A.; Tournier, N.; Mériaux, S.; Larrat, B. Regulation of P-glycoprotein and breast cancer resistance protein expression induced by focused ultrasound-mediated blood-brain barrier disruption. *Int. J. Mol. Sci.* **2022**, *22*, x. https://doi.org/10.3390/xxxxx

Academic Editor:

Received: date
Accepted: date
Published: date

1. Introduction

The blood-brain barrier (BBB) prevents macromolecules, small organic drugs, and ions from entering the brain, and it constitutes a major limit to central nervous system (CNS) pharmacotherapy [1,2]. The BBB comprises mainly endothelial cells connected by tight junctions (TJs) that, together with efflux transporters, can restrict the passage of substrate molecules from the blood circulation to the brain [3–6]. ATP-binding cassette (ABC) transporters such as the P-glycoprotein (P-gp) and breast cancer resistance protein (BCRP) are expressed at the BBB. Both P-gp and BRCP further minimize the transport of a large amount of drugs to the brain, as observed with anti-epileptic and anticancer drugs [5,7]. The P-gp and BCRP work in synergy, so the brain uptake of dual P-gp/BCRP substrates increases only when both P-gp and BCRP are down-regulated simultaneously. Indeed, if only one of the two pumps is down-regulated, compensation by the other may occur which still limits the molecular transport from the blood to the brain [8]. For example, it has been demonstrated that administering P-gp inhibitors can lead to an overall expression of BCRP [9].

Various approaches have been proposed to overcome BBB-related drug delivery challenges [10]. Among them, low-intensity focused ultrasound (FUS, typically referred to intensities of the order of 1 W/cm^2 *in situ*, compatible with acoustic pressures below 1.5 MPa) combined with circulating microbubbles (MBs) is a non-invasive technique that offers superior target specificity. The microbubble cavitation induced by FUS can act mechanically on the TJs, creating reversible gaps in the endothelial walls [11–15], through which passive transport of macromolecules to the brain is increased in a controlled and safe manner [16–22]. Few studies have suggested that BBB opening by FUS may also cause temporary down-expression of P-gp on vessel walls, the duration of which was dependent on acoustic pressure (AP). P-gp was shown to fully recover three days after FUS application at low AP (e.g., peak negative pressure – PNP of 0.5 MPa, *in situ*) [23,24] whereas, at a higher AP of 0.8 MPa (similar to levels used in brain tumors trials [25,26]), P-gp does not return to baseline after three days [24]. However, despite these early findings, very little is known about the joint dynamics of FUS-induced regulation of efflux transporters expressed at the BBB, and more data is needed to compare the dynamics of the expression of P-gp and BCRP over a longer time after FUS. This pilot study aims to bridge these gaps by investigating, for the first time the effects of FUS-mediated BBB-opening on P-gp and BCRP expressions at 0.8 MPa over 14 days.

2. Results

Figure 1 shows representative P-gp/BCRP stainings of sonicated and contralateral brain tissues obtained on days one and fourteen after FUS-induced BBB disruption. After BBB disruption, P-gp is down-regulated at day one compared to BCRP and 14 days after sonication. At no timepoints, BCRP is downregulated by FUS. Further protein stainings confirming these results are shown in the supplementary materials (Figures S1-S4).

The levels of each differentially expressed protein up to 14 days after FUS are shown in figure 2 for both brain hemispheres (sonicated vs. contralateral). Three animals were used to assess the expression of each protein at each time point. For each animal, protein expressions were assessed in two slices centered in the focal spot region, with three ROIs per animal for each hemisphere, yielding a total of 18 ROIs for each time point.

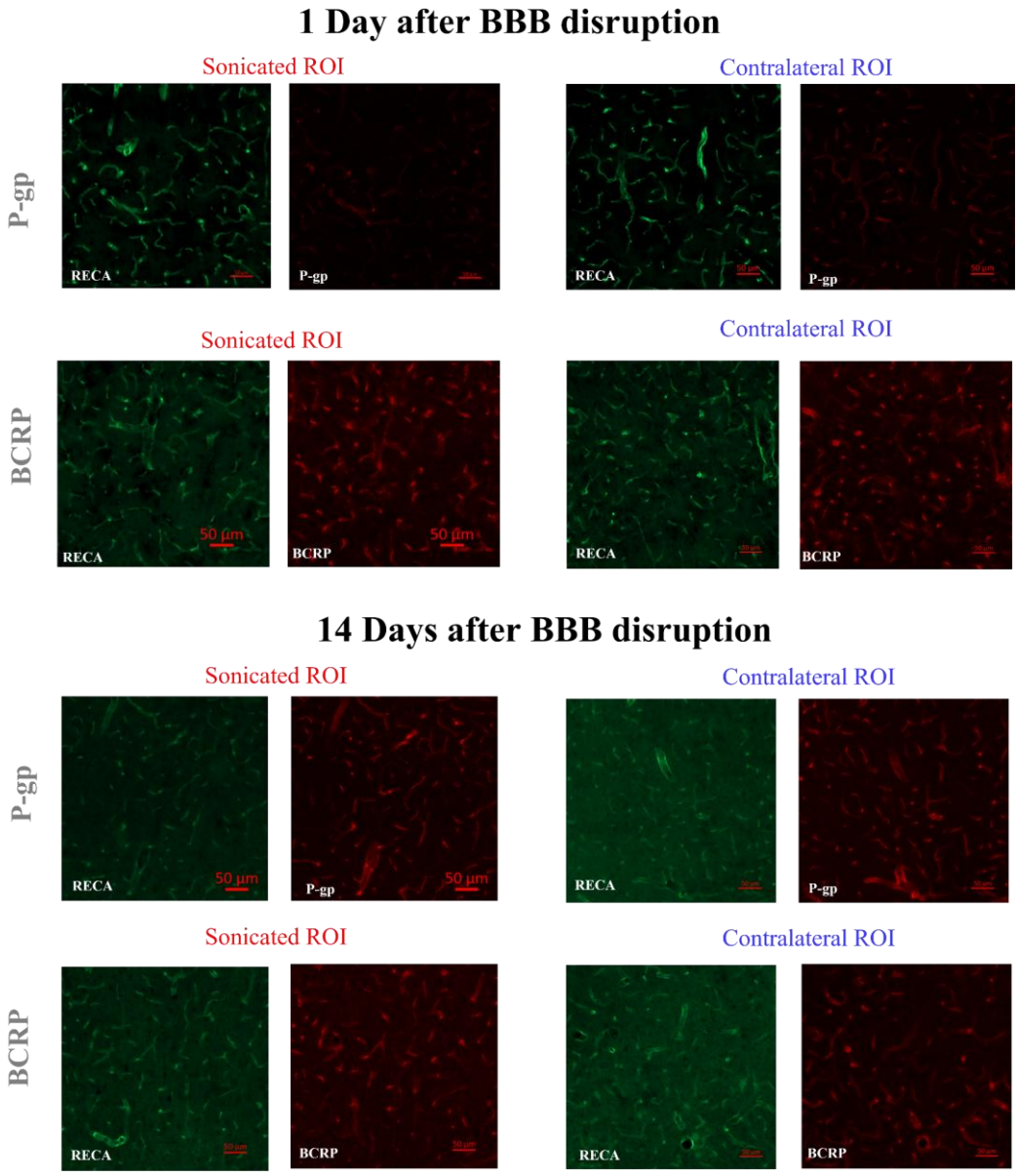

Figure 1. Representative immunohistochemical staining of P-gp and BCRP on sonicated and contralateral brain tissues, obtained at one and fourteen days after FUS-induced BBB disruption.

Although the median P-gp expression in sonicated regions appears lower than in contralateral regions, such differences are not statistically significant, as shown in Table 1. These findings suggest that AP of 0.8 MPa affects P-gp expression throughout the brain with signs of increased effects on the sonicated side.

When comparing P-gp expression in the sonicated or contralateral regions at different time points, it is possible to detect statistically significant changes in this protein expression over time. The p-values resulting from all statistical comparisons in sonicated and contralateral ROIs are shown in Tables 2 and 3, respectively. Our findings imply that one day after sonication, P-gp expression is lower in both sonicated and contralateral regions than in the following days ($p<0.05$ from all comparisons between day one and day three and seven, performed in single hemispheres separately). In addition, P-gp expression did not change from day three to day fourteen in both hemispheres.

Regarding BCRP, the results of Mann-Whitney U tests suggest that:

i) Up to seven days after sonication, BCRP is significantly higher in the sonicated area compared with the contralateral brain regions (p-values fdr corrected<0.05, Table 1);

ii) Two weeks after sonication, BCRP expression in the treated and untreated regions is similar (p-value fdr corrected>0.05 when comparing hemispheres at day 14);

iii) BCRP expression remains constant in the two hemispheres within a week after FUS (p-values fdr corrected>0.05 from all comparisons between time points, Table 2 and 3).

iv) Interestingly, in the sonicated regions, BCRP appears to be significantly more expressed for the first seven days compared with two weeks post-FUS (Table 2). The same effect was not observed on the contralateral side (Table 3).

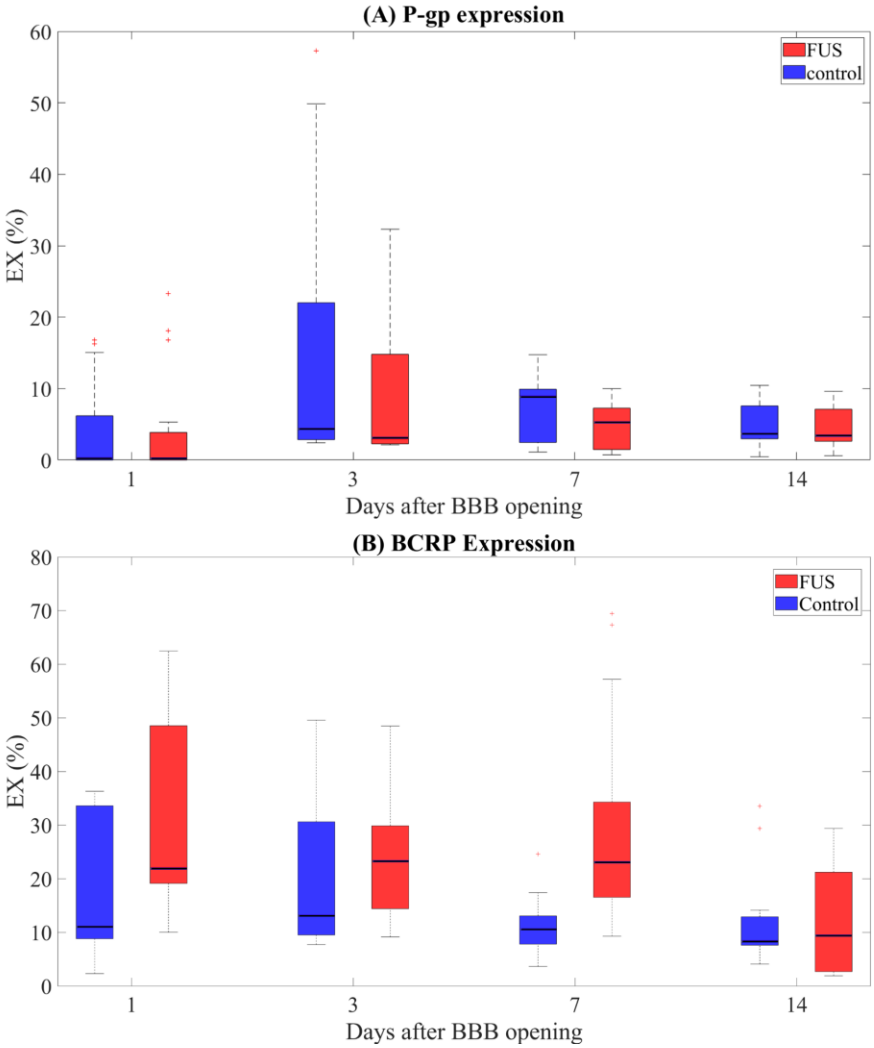

Figure 2. P-gp and BCRP expressions evaluated in 18 ROIs/time points in both sonicated (in red) and contralateral untreated brain regions (in blue).

Table 1. p-values resulting from Mann-Whitney tests performed to compare P-gp and BCRP expressions between sonicated and contralateral brain regions at 1, 3, 7, and 14 days after FUS application (18 ROIs per brain hemisphere, at each time point). P-values were corrected for multiple comparisons (fdr, alpha=0.05).

P-gp Expression		BCRP Expression	
Days After Sonication	**p-Value**	**Days After Sonication**	**p-Value**
Day 1	0.88	Day 1	0,028*
Day 3	0.46	Day 3	0,5
Day 7	0.22	Day 7	2,52e-4*
Day 14	0.93	Day 14	0,93

Table 2. p-values from comparing P-gp and BCRP expressions in 18 sonicated ROIs at all time points. P-values were corrected for multiple comparisons (fdr, alpha=0.05).

P-gp Expression		BCRP Expression	
Comparison	**p-Value**	**Comparison**	**p-Value**
Day 1/Day 3	6.8e-3*	Day 1/Day 3	0.51
Day 1/Day 7	6.8e-3*	Day 1/Day 7	1.00
Day 1/ Day 14	0.02*	Day 1/ Day 14	3.0E-03*
Day 3/ Day 7	0.51	Day 3/ Day 7	0.50
Day 3/ Day 14	0.51	Day 3/ Day 14	1.36E-02*
Day 7/ Day 14	0.93	Day 7/ Day 14	3.00e-3*

Table 3. p-values from comparing P-gp and BCRP expressions in 18 contralateral ROIs at all time points. P-values were corrected for multiple comparisons (fdr, alpha=0.05).

P-gp Expression		BCRP Expression	
Comparison	**p-Value**	**Comparison**	**p-Value**
Day 1/Day 3	4.80e-3*	Day 1/Day 3	0.74
Day 1/Day 7	1.10e-2*	Day 1/Day 7	0.32
Day 1/ Day 14	0.064	Day 1/ Day 14	0.26
Day 3/ Day 7	0.48	Day 3/ Day 7	0.104
Day 3/ Day 14	0.51	Day 3/ Day 14	0.064
Day 7/ Day 14	0.36	Day 7/ Day 14	0.69

Figure 3 shows the percentage of voxels (EXr (%)) expressing P-gp or BCRP in sonicated tissues compared to the contralateral hemispheres. BCRP expression is

significantly higher than P-gp expression within a week after BBB disruption (all p-values<0.05 when comparing their expressions at 1, 3, and 7 days after sonication), while their expressions are similar at two weeks after FUS application (p-value=0.57).

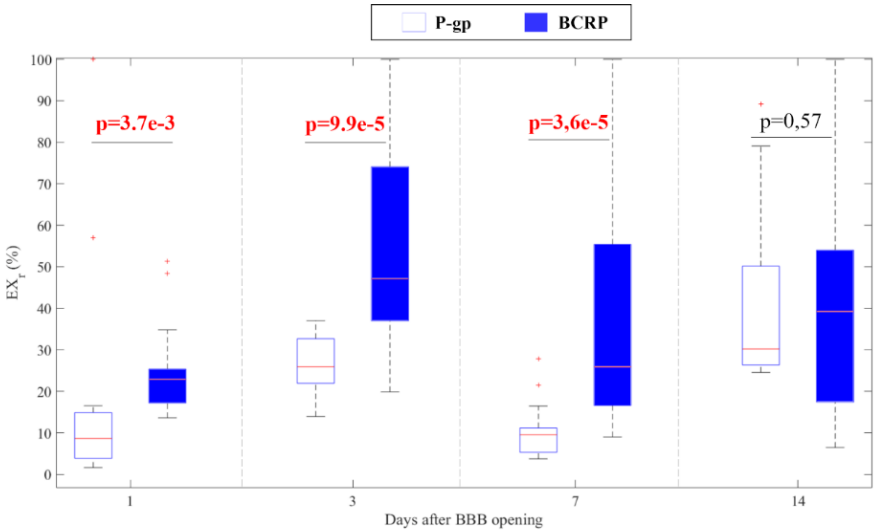

Figure 3. Boxplots of both P-gp and BCRP expressions in the sonicated regions normalized to the expressions in the contralateral ROIs evaluated at different time points within two weeks after FUS application.

3. Discussion and conclusions

In this pilot study, we investigated for the first time the impact of FUS-mediated BBB disruption at moderate AP on the expression of both P-gp and BCRP for up to 2 weeks post-sonication. Our results show that at 0.8 MPa, P-gp is down-expressed for up to 3 days after sonication. In addition, corroborating a previous study [24], this transport is down-regulated in the treated region and the contralateral hemisphere. On the contrary, BCRP was over-expressed in the treated regions only for up to seven days after FUS application and fully recovered within two weeks. Overall, these results suggest that i) FUS can alter the expressions of P-gp but also impacts BCRP; ii) full recovery is achieved within two weeks.

3.1. Implications in drug delivery strategies

Our findings can help shed light on the biological mechanisms induced by FUS and explain why, in some cases, it cannot improve molecular uptake in the brain. Even at optimal post-FUS times (i.e., when the P-gp is maximally inhibited), P-gp down-expression may remain insufficient to block its function [27]. In addition, our results show that P-gp inhibition is accompanied by BCRP over-expression that compensates for P-gp partial loss of action. This suggests that administering inhibitors of BCRP proteins in conjunction with FUS application may be beneficial for further enhancing molecular delivery to the brain of ABC transporter substrate molecules (such as tyrosine kinase inhibitors). In addition, investigating the impact of FUS on brain tumors where this transporter is over-expressed may help offer alternative mechanisms to fight the disease [28–30]. For example, it may inspire new drug designs based on delivery strategies in this framework. Indeed, our preliminary results suggest that this method may improve the delivery of substrates of P-gp that are not substrates of BCRP, which FUS overexpresses.

3.2. Study limitations and future directions

This is the first study demonstrating that FUS-induced BBB disruption is accompanied by dysregulation of both P-gp and BCRP, the main efflux transporters at the BBB, in opposite directions. Future studies should be conducted with a larger animal cohort to increase the statistical power of the results.

Here we set out to understand the acute and very focal effects of FUS application targeted to a single point in the brain (i.e., a protocol typically found in clinical applications [26, 34]). The limited brain volume (2 x 2 x 6 mm^3) exposed to the same acoustic energy did not allow us to assess P-gp and BCRP expression using immunohistochemistry in conjunction with western blot. For our purposes, the study design also allowed a cross-comparison of our results with a previous study showing the effects n of the same acoustic intensity on P-gp expression [24].

Future studies, investigating the effects of FUS on a much larger sonication volume (e.g., whole thalamus [23]), will allow protein expressions to be assessed by immunohistochemistry along with more quantitative methods (e.g., western blot).

In addition, since the permeabilization of the BBB under FUS strongly depends on the acoustic parameters used during sonication (e.g., AP, FUS frequency, duty cycle) as well as the type of MBs, further studies are needed to investigate the functional impact of these parameters on the expression of both efflux transporters. The generalization of the present findings obtained on rodents to other mammalian brains, including human beings, also remains an open question since it is known that ABC transporter expressions vary among species.

4. Materials and Methods

4.1. Animals

All experiments were performed in accordance with the recommendations of the European Community (86/609/EEC) and the French legislation (decree no. 87/848) for the use and care of laboratory animals. All animal experiments were approved by the Comité d'Éthique en Expérimentation Animale du Commissariat à l'Énergie Atomique et aux énergies alternatives Direction des Sciences du Vivant Ile de France (CETEA CEA DSV IdF) under protocol ID_ 12-058. Experiments were performed on 12 Fischer male rats (~350 g). Animals were anesthetized by using a mixture of air, oxygen, and 1.5% isoflurane and head shaved before being placed in the MRgFUS device. A heater was used to keep the animals close to their physiologic temperature of 36±1°C. Body temperature and respiration rate were continuously monitored during the experiments. A catheter was inserted in the caudal vein to inject both microbubbles and MRI contrast agent (CA) from outside the scanner.

4.2. Experimental protocol

The experimental protocol is depicted in figure 4, along with timelines for the BBB permeabilization procedure and MRI acquisition. After the installation of the animals in the MRI scanner (7 T / 90 mm bore hole Pharmascan scanner, Bruker, Ettlingen, Germany), Acoustic Radiation Force Imaging (ARFI) [31] was acquired to confirm FUS targeting in the brain (MSME, TE/TR=28/1080 ms, matrix=64x64x5, res=0.5x0.5x2mm^3, total duration: 2'30''). T_1-weighted images where then acquired (T_1-w, MSME sequence, TE/TR = 8.3/300 ms, matrix dimension = 256×256×10, resolution= 0.125×0.125×1 mm^3, 3 averages, acquisitions time= 2 min) before FUS application. The acoustic treatment consisted of 3 ms bursts, every 100 ms over a period of one minute, with an estimated focal PNP in the brain of 0.8 MPa, taking into account skull transmission factor based on [32]. An AP of 0.8 MPa was chosen since it is a typical level used to permeabilize the BBB in brain tumors in preclinical and clinical trials [25,26]. The treatment was performed with an MR-compatible FUS transducer (1.5 MHz central frequency, diameter: 25 mm, focal depth: 20 mm, Imasonic, France) connected to a therapeutic programmable FUS generator (Image-Guided Therapy, Pessac, France).

FUS was applied at a single point in the striatum (focal spot- FS: 2×2×6 mm^3) [33]. A 200 µL bolus of SonoVue microbubbles (Bracco, Italy) was injected via a tail-vein catheter approximately 5s before sonication. Approximately 30 seconds after FUS application, a Gadolinium-based CA (Dotarem®, 1 nm diameter, 1.6 mL/kg) was injected via catheter. Approximately 30 seconds after the CA-administration T_1-w acquisition started. At the end of each experimental session, T_2-weighted (T2-w) images were acquired through a RARE sequence (TE/TR=10/3800 ms, RARE factor=8, matrix=128x128x32, res=0.225x0.225x0.5 mm^3) to verify the absence of any hemorrhage or edema due to the BBB permeabilization proto

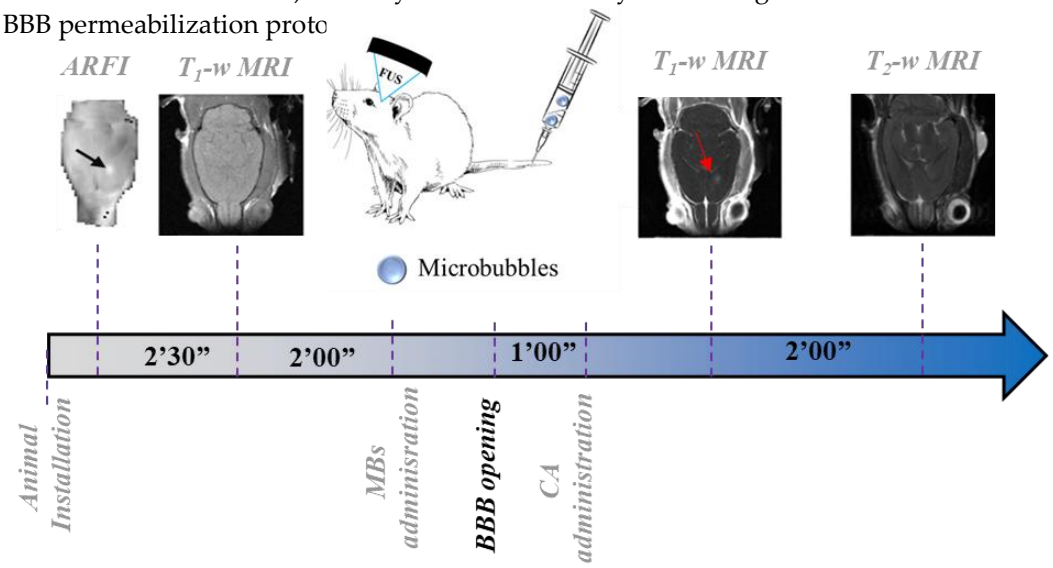

Figure 4. Experimental protocol for *in vivo* experiments and timelines for the BBB permeabilization procedure and MRI acquisition. After the installation of the animal in the MRI scanner, the position of the FUS focal spot was confirmed with an MR-ARFI sequence. This acquisition was then followed by a T_1-w scan acquired before BBB opening. One minute after FUS application, and MRI-CA administration, T1-w (2 min acquisition) and T2-w (2 min) images were acquired to evaluate the extension of the BBB disruption and the presence of damages, respectively.

4.3. Immunohistochemistry

BCRP and P-gp expressions were evaluated through histology performed on three rats per each time point at 1, 3, 7, and 14 days after BBB opening. Extracted brains were sliced using a microtome (slices thickness=30 µm). Endothelial cells were stained by RECA-1 antibody (mouse anti-RECA-1 from Abcam, ab9774, diluted at 1/2000), while P-gp and BCRP expressions were evaluated through rabbit anti-P-gp (Abcam ab170904, diluted at 1/100) and rabbit anti-BCRP from Abcam ab207732 (diluted at 1/100) all used after antigen retrieval process (acetic acid 33%/ethanol pure 66%; 10 min -30°C) and the block of permeabilization process (Donkey serum 5% +BSA 1% + triton 1%). Representative negative controls of immuno-stained regions are shown in figure S5. For each double staining P-gp/RECA-1 and BCRP/RECA-1, brain slides were processed through the following protocol:

1. Wash 2x5min with PBS (concentration of 0.01M);
2. Application of antigen retrieval process (ac/eth) followed by blocking/permeabilization protocols (2 hours);
3. Wash with PBS;
4. Incubation of the first antibody (1 hour for P-gp / 2 hours for BCRP);
5. Wash 2x5min with PBS;
6. Incubation of the RECA-1 antibody for 1 hour;
7. Wash 2x5min with PBS;

8. Incubation for 1 hour of secondary Dk anti-Rabbit Alexa647 and the secondary Dk anti-mouse Dylight488;
9. Wash 3x5min with PBS;
10. Application of ProLong with Dapi (mounting media, from ThermoFisher, ref P36931).

Histological images were obtained using an AxioObserver Z1 microscope (Zeiss, Germany) with an MRm camera and analyzed using Carl Zeiss AxioVision software. Mozaic scans cover the fields of view through the Tile function of the software.

4.4. Histological findings evaluation

Figure 5 shows the pipeline used to evaluate histological findings quantitatively:

1. First, the center of the BBB opening was identified in all rat brains by looking at T_1-w images acquired immediately after FUS application and CA injection (Fig.5(A)).
2. Four brain slices positioned around the center of the FUS focal spot were stained for both RECA-1/P-gp (2 slices) and RECA-1/BCRP (2 slices), as shown in Fig.5(B-C).
3. A custom MATLAB script (MathWorks, USA) thresholded and binarized histological images for all stainings, as follows (Fig.5(D)):
   i. distributions of P-gp/BCRP and RECA expressions were first fitted in the red and green color channels, respectively, through Gaussian functions. The mean (M) and the standard deviation (σ) of each of these distributions were calculated.
   ii. Binarized images were obtained by excluding hyper/hypointense meaningless background voxels (i.e., with values lower than [M - 2.5σ] or higher than [M+2.5σ]).
4. For each slice and staining, three adjacent square Regions of Interest (ROIs) of 1000 voxels side (about 2 mm) centered on the focal spot and the contra-lateral side were defined (fig.5(E)). The ROIs were chosen to be large enough to cover the ultrasound spot dimensions (2 mm wide, 6 mm long). Finally, this led us to 6 analyzed ROIs per staining and per rat (18 ROIs in total per single hemisphere/time point). Our sample size was similar to that used in [24], so that we had sufficient statistical power to assess the effects of FUS on the expression of both proteins.
5. In order to remove remaining spurious noisy voxels, the voxels in each of these ROIs were clustered using a custom MATLAB code (fig.5(F)). The value of the suprathreshold voxel among eight neighbors was assigned to one cluster. This technique was used for all BCRP, P-gp, and RECA-1 stainings.
6. The expressions of P-gp and BCRP were defined as the percentage of voxels in each ROI expressing both proteins (P-gp or BCRP) and RECA-1. These voxels are depicted in blue in fig.5(G) for a representative ROI in which both P-gp and RECA-1 were expressed.

To assess the effects of FUS on the expressions of BCRP and P-gp at different time points, the percentage of voxels expressing the two proteins was compared to the

contralateral hemisphere ($EX_r(\%) = \frac{EX_u}{EX_c} \cdot 100$).

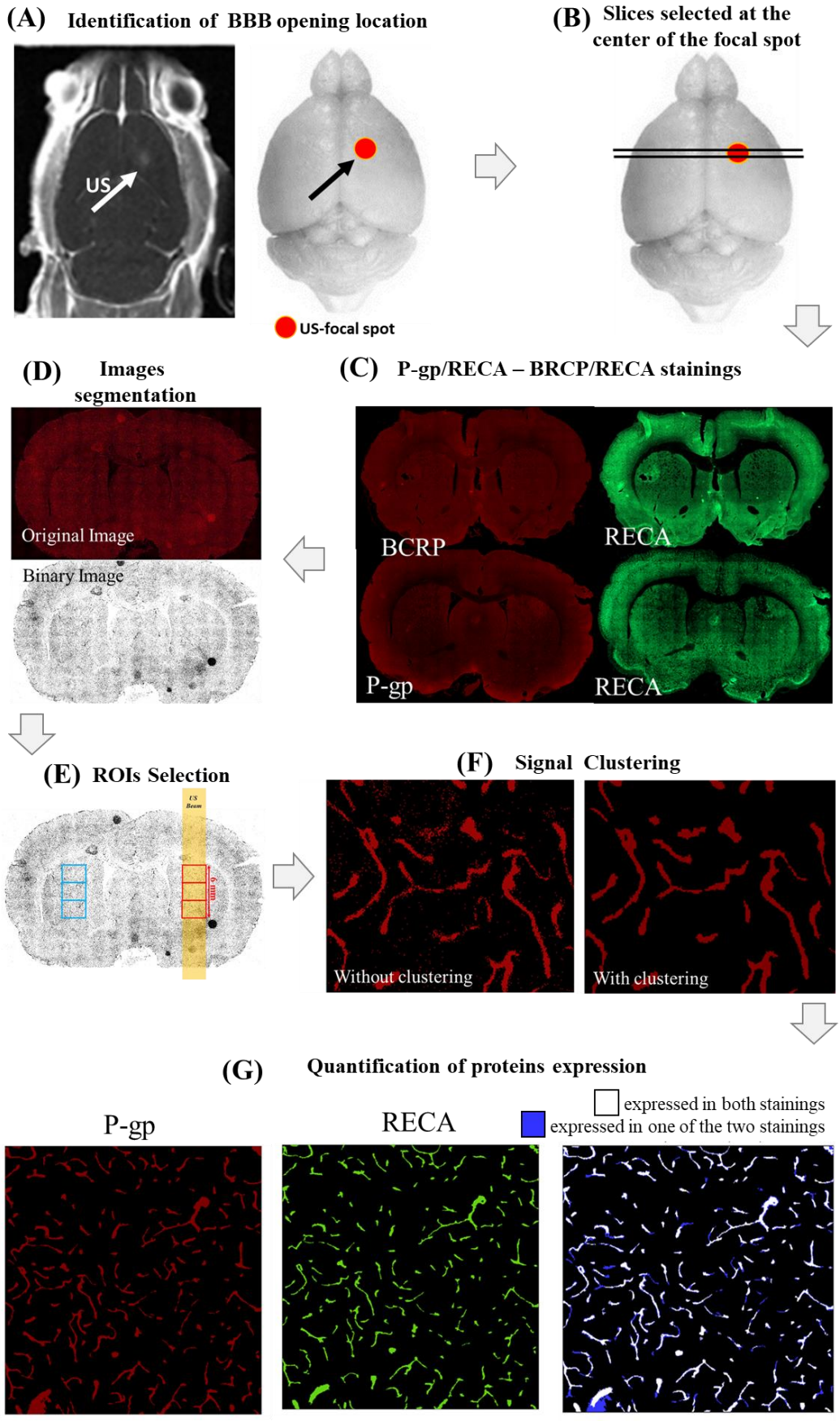

Figure 5. Pipeline used to evaluate P-gp, BCRP, and RECA expressions in rat brain after FUS. In all cases, the center of the focal spot was identified in post-contrast T_1-w images acquired right after BBB disruption and MRI-CA administration (A). (B): 4 slices centered in the focal regions were selected (all of them were stained with RECA, while groups of two slices were stained with P-gp and RECA, respectively). Figure (C) shows two representative slices (one per protein) with the respective RECA stainings. All slices were binarized (D), then three squared regions (2 mm wide) were selected at the center of the focal spot, both in the sonicated and contralateral hemispheres (E). Expressions in all ROIs were clustered to remove voxels belonging to the background (F). As the last step, the expression of each protein was evaluated as the percentage of voxels expressing both RECA-1 and BCRP or P-gp (blue voxels in fig. (G)).

4.5. Statistical Analysis

A Mann-Whitney U test was used to assess protein expression in sonicated and untreated contralateral brain hemispheres at 1, 3, 7, and 14 days after FUS. Furthermore, using the same statistical approach, P-gp/BCRP expressions were independently compared between these time points in the sonicated and contralateral ROIs. P-values were then corrected for multiple comparisons (four Mann-Whitney tests on each dataset by considering comparisons across hemispheres and time points). A false discovery rate (fdr) correction was applied to account for multiple comparisons (alpha=0.05). A Mann-Whitney U test was also used to compare EXr values relative to P-gp and BCRP expressions at all time points. For all statistical tests, protein expression differences were considered statistically significant for p-values smaller than 0.05.

Author Contributions: AC and BL planned the MRI experiments. AC and HK performed MRI acquisitions and BBB opening experiments. SM provided MRI data analysis pipelines. FG collected histological data. AC performed data analysis. AC and BL managed the overall project. All authors contributed to the manuscript edition.

Funding: Research supported by Enhanced Eurotalents post-doctoral fellowship (Grant Agreement n°600382), part of the Marie Sklodowska-Curie Actions Program, co-funded by the European Commission and managed by the French Atomic Energy and Alternative Energies Commission (CEA).

Institutional Review Board Statement: All animal experiments were approved by the Comité d'Éthique en Expérimentation Animale du Commissariat à l'Énergie Atomique et aux énergies alternatives Direction des Sciences du Vivant Ile de France (CETEA CEA DSV IdF) under protocol ID_ 12-058, site authorization number: B-91-272-01.

Data Availability Statement: The data presented in this study are available on request from the corresponding author.

Conflicts of Interest: The authors declare that the research was conducted in the absence of any commercial or financial relationships that could be construed as a potential conflict of interest.

References

1. Miller, D.S.; Bauer, B.; Hartz, A.M.S. Modulation of P-Glycoprotein at the Blood-Brain Barrier: Opportunities to Improve CNS Pharmacotherapy. *Pharmacol Rev* **2008**, *60*, 196–209, doi:10.1124/pr.107.07109.
2. Daneman, R.; Prat, A. The Blood-Brain Barrier. *Cold Spring Harb Perspect Biol* **2015**, *7*, a020412, doi:10.1101/cshperspect.a020412.
3. Laksitorini, M.; Prasasty, V.D.; Kiptoo, P.K.; Siahaan, T.J. Pathways and Progress in Improving Drug Delivery through the Intestinal Mucosa and Blood-Brain Barriers. *Ther Deliv* **2014**, *5*, 1143–1163, doi:10.4155/tde.14.67.
4. Begley, D.J. ABC Transporters and the Blood-Brain Barrier. *Curr Pharm Des* **2004**, *10*, 1295–1312, doi:10.2174/1381612043384844.
5. Löscher, W.; Potschka, H. Blood-Brain Barrier Active Efflux Transporters: ATP-Binding Cassette Gene Family. *NeuroRx* **2005**, *2*, 86–98.
6. Rhea, E.M.; Banks, W.A. Role of the Blood-Brain Barrier in Central Nervous System Insulin Resistance. *Frontiers in Neuroscience* **2019**, *13*.

7. Arif, W.M.; Elsinga, P.H.; Gasca-Salas, C.; Versluis, M.; Martínez-Fernández, R.; Dierckx, R.A.J.O.; Borra, R.J.H.; Luurtsema, G. Focused Ultrasound for Opening Blood-Brain Barrier and Drug Delivery Monitored with Positron Emission Tomography. *Journal of Controlled Release* **2020**, *324*, 303–316, doi:10.1016/j.jconrel.2020.05.020.
8. Agarwal, S.; Sane, R.; Ohlfest, J.R.; Elmquist, W.F. The Role of the Breast Cancer Resistance Protein (ABCG2) in the Distribution of Sorafenib to the Brain. *J Pharmacol Exp Ther* **2011**, *336*, 223–233, doi:10.1124/jpet.110.175034.
9. Lee, J.; Kang, J.; Kwon, N.-Y.; Sivaraman, A.; Naik, R.; Jin, S.-Y.; Oh, A.R.; Shin, J.-H.; Na, Y.; Lee, K.; et al. Dual Inhibition of P-Gp and BCRP Improves Oral Topotecan Bioavailability in Rodents. *Pharmaceutics* **2021**, *13*, 559, doi:10.3390/pharmaceutics13040559.
10. Hersh, D.S.; Wadajkar, A.S.; Roberts, N.; Perez, J.G.; Connolly, N.P.; Frenkel, V.; Winkles, J.A.; Woodworth, G.F.; Kim, A.J. Evolving Drug Delivery Strategies to Overcome the Blood Brain Barrier. *Curr Pharm Des* **2016**, *22*, 1177–1193.
11. Hynynen, K.; McDannold, N.; Vykhodtseva, N.; Jolesz, F.A. Noninvasive MR Imaging-Guided Focal Opening of the Blood-Brain Barrier in Rabbits. *Radiology* **2001**, *220*, 640–646, doi:10.1148/radiol.2202001804.
12. Marty, B.; Larrat, B.; Van Landeghem, M.; Robic, C.; Robert, P.; Port, M.; Le Bihan, D.; Pernot, M.; Tanter, M.; Lethimonnier, F.; et al. Dynamic Study of Blood-Brain Barrier Closure after Its Disruption Using Ultrasound: A Quantitative Analysis. *J Cereb Blood Flow Metab* **2012**, *32*, 1948–1958, doi:10.1038/jcbfm.2012.100.
13. Samiotaki, G.; Konofagou, E.E. Dependence of the Reversibility of Focused- Ultrasound-Induced Blood-Brain Barrier Opening on Pressure and Pulse Length in Vivo. *IEEE Trans Ultrason Ferroelectr Freq Control* **2013**, *60*, 2257–2265, doi:10.1109/TUFFC.2013.6644731.
14. Sun, T.; Samiotaki, G.; Wang, S.; Acosta, C.; Chen, C.C.; Konofagou, E.E. Acoustic Cavitation-Based Monitoring of the Reversibility and Permeability of Ultrasound-Induced Blood-Brain Barrier Opening. *Phys Med Biol* **2015**, *60*, 9079–9094, doi:10.1088/0031-9155/60/23/9079.
15. Conti, A.; Mériaux, S.; Larrat, B. About the Marty Model of Blood-Brain Barrier Closure after Its Disruption Using Focused Ultrasound. *Phys Med Biol* **2019**, *64*, 14NT02, doi:10.1088/1361-6560/ab259d.
16. Konofagou, E.E.; Tung, Y.-S.; Choi, J.; Deffieux, T.; Baseri, B.; Vlachos, F. Ultrasound-Induced Blood-Brain Barrier Opening. *Curr Pharm Biotechnol* **2012**, *13*, 1332–1345, doi:10.2174/138920112800624364.
17. Sheikov, N.; McDannold, N.; Vykhodtseva, N.; Jolesz, F.; Hynynen, K. Cellular Mechanisms of the Blood-Brain Barrier Opening Induced by Ultrasound in Presence of Microbubbles. *Ultrasound Med Biol* **2004**, *30*, 979–989, doi:10.1016/j.ultrasmedbio.2004.04.010.
18. McDannold, N.; Vykhodtseva, N.; Hynynen, K. Blood-Brain Barrier Disruption Induced by Focused Ultrasound and Circulating Preformed Microbubbles Appears to Be Characterized by the Mechanical Index. *Ultrasound Med Biol* **2008**, *34*, 834–840, doi:10.1016/j.ultrasmedbio.2007.10.016.
19. Park, J.; Zhang, Y.; Vykhodtseva, N.; Akula, J.D.; McDannold, N.J. Targeted and Reversible Blood-Retinal Barrier Disruption via Focused Ultrasound and Microbubbles. *PLOS ONE* **2012**, *7*, e42754, doi:10.1371/journal.pone.0042754.
20. Samiotaki, G.; Vlachos, F.; Tung, Y.-S.; Konofagou, E.E. A Quantitative Pressure and Microbubble-Size Dependence Study of Focused Ultrasound-Induced Blood-Brain Barrier Opening Reversibility in Vivo Using MRI. *Magn Reson Med* **2012**, *67*, 769–777, doi:10.1002/mrm.23063.
21. Fan, C.-H.; Yeh, C.-K. Microbubble-Enhanced Focused Ultrasound-Induced Blood–Brain Barrier Opening for Local and Transient Drug Delivery in Central Nervous System Disease. *Journal of Medical Ultrasound* **2014**, *22*, 183–193, doi:10.1016/j.jmu.2014.11.001.
22. Kamimura, H.A.; Flament, J.; Valette, J.; Cafarelli, A.; Aron Badin, R.; Hantraye, P.; Larrat, B. Feedback Control of Microbubble Cavitation for Ultrasound-Mediated Blood–Brain Barrier Disruption in Non-Human Primates under Magnetic Resonance Guidance. *J Cereb Blood Flow Metab* **2019**, *39*, 1191–1203, doi:10.1177/0271678X17753514.
23. Choi, H.; Lee, E.-H.; Han, M.; An, S.-H.; Park, J. Diminished Expression of P-Glycoprotein Using Focused Ultrasound Is Associated With JNK-Dependent Signaling Pathway in Cerebral Blood Vessels. *Frontiers in Neuroscience* **2019**, *13*.
24. Aryal, M.; Fischer, K.; Gentile, C.; Gitto, S.; Zhang, Y.-Z.; McDannold, N. Effects on P-Glycoprotein Expression after Blood-Brain Barrier Disruption Using Focused Ultrasound and Microbubbles. *PLoS One* **2017**, *12*, e0166061, doi:10.1371/journal.pone.0166061.
25. Mungur, R.; Zheng, J.; Wang, B.; Chen, X.; Zhan, R.; Tong, Y. Low-Intensity Focused Ultrasound Technique in Glioblastoma Multiforme Treatment. *Frontiers in Oncology* **2022**, *12*.
26. Idbaih, A.; Canney, M.; Belin, L.; Desseaux, C.; Vignot, A.; Bouchoux, G.; Asquier, N.; Law-Ye, B.; Leclercq, D.; Bissery, A.; et al. Safety and Feasibility of Repeated and Transient Blood–Brain Barrier Disruption by Pulsed Ultrasound in Patients with Recurrent Glioblastoma. *Clinical Cancer Research* **2019**, *25*, 3793–3801, doi:10.1158/1078-0432.CCR-18-3643.
27. Goutal, S.; Gerstenmayer, M.; Auvity, S.; Caillé, F.; Mériaux, S.; Buvat, I.; Larrat, B.; Tournier, N. Physical Blood-Brain Barrier Disruption Induced by Focused Ultrasound Does Not Overcome the Transporter-Mediated Efflux of Erlotinib. *J Control Release* **2018**, *292*, 210–220, doi:10.1016/j.jconrel.2018.11.009.
28. Rabkin, D.; Chhieng, D.C.; Miller, M.B.; Jennings, T.; Feustel, P.; Steiniger, J.; Parnes, S.M. P-Glycoprotein Expression in the Squamous Cell Carcinoma of the Tongue Base. *Laryngoscope* **1995**, *105*, 1294–1299, doi:10.1288/00005537-199512000-00006.

29. Iorio, A.L.; da Ros, M.; Fantappiè, O.; Lucchesi, M.; Facchini, L.; Stival, A.; Becciani, S.; Guidi, M.; Favre, C.; de Martino, M.; et al. Blood-Brain Barrier and Breast Cancer Resistance Protein: A Limit to the Therapy of CNS Tumors and Neurodegenerative Diseases. *Anticancer Agents Med Chem* **2016**, *16*, 810–815, doi:10.2174/1871520616666151120121928.
30. Arvanitis, C.D.; Ferraro, G.B.; Jain, R.K. The Blood–Brain Barrier and Blood–Tumour Barrier in Brain Tumours and Metastases. *Nat Rev Cancer* **2020**, *20*, 26–41, doi:10.1038/s41568-019-0205-x.
31. Larrat, B.; Pernot, M.; Aubry, J.-F.; Dervishi, E.; Sinkus, R.; Seilhean, D.; Marie, Y.; Boch, A.-L.; Fink, M.; Tanter, M. MR-Guided Transcranial Brain HIFU in Small Animal Models. *Phys Med Biol* **2010**, *55*, 365–388, doi:10.1088/0031-9155/55/2/003.
32. Gerstenmayer, M.; Fellah, B.; Magnin, R.; Selingue, E.; Larrat, B. Acoustic Transmission Factor through the Rat Skull as a Function of Body Mass, Frequency and Position. *Ultrasound in Medicine & Biology* **2018**, *44*, 2336–2344, doi:10.1016/j.ultrasmedbio.2018.06.005.
33. Magnin, R.; Rabusseau, F.; Salabartan, F.; Mériaux, S.; Aubry, J.-F.; Le Bihan, D.; Dumont, E.; Larrat, B. Magnetic Resonance-Guided Motorized Transcranial Ultrasound System for Blood-Brain Barrier Permeabilization along Arbitrary Trajectories in Rodents. *J Ther Ultrasound* **2015**, *3*, 22, doi:10.1186/s40349-015-0044-5.
34. Roberts, J. W., Powlovich L., Sheybani N. and LeBlang S. Focused ultrasound for the treatment of glioblastoma. *J Neurooncol* **2022**, 157, 2, 237–247, doi: 10.1007/s11060-022-03974-0